
Intertidal limits shape covariation between metabolic plasticity, oxidative stress and telomere dynamics in Pacific oyster (*Crassostrea gigas*)

Dupoué Andréaz ^{1,*}, Ferraz Mello Trevisan Danielle ¹, Trevisan Rafael ^{1,2}, Dubreuil Christine ¹, Queau Isabelle ¹, Petton Sébastien ¹, Huvet Arnaud ¹, Guével Blandine ^{3,4}, Com Emmanuelle ^{3,4}, Pernet Fabrice ¹, Salin Karine ¹, Fleury Elodie ¹, Corporeau Charlotte ¹

¹ Ifremer, Univ Brest, CNRS, IRD, UMR 6539, LEMAR, F-29280, Plouzane, France

² Laboratoire Environnement Ressources Bretagne Occidentale (LER/BO), Ifremer, 29900, Concarneau, France

³ Univ Rennes, Inserm, EHESP, Irset (Institut de Recherche en Santé, Environnement et Travail) - UMR_S 1085, F-35000, Rennes, France

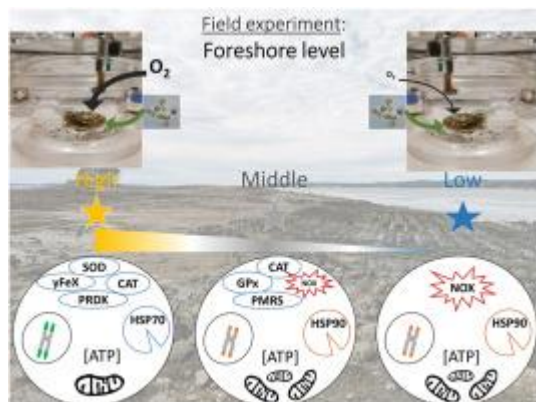
⁴ Univ Rennes, CNRS, Inserm, Biosit UAR 3480 US_S 018, Protim Core Facility, F-35000, Rennes, France

* Corresponding author : Andréaz Dupoué, email address : andreaz.dupoue@gmail.com

Abstract :

In intertidal zones, species such as sessile shellfish exhibit extended phenotypic plasticity to face rapid environmental changes, but whether frequent exposure to intertidal limits of the distribution range impose physiological costs for the animal remains elusive. Here, we explored how phenotypic plasticity varied along foreshore range at multiple organization levels, from molecular to cellular and whole organism acclimatization, in the Pacific oyster (*Crassostrea gigas*). We exposed 7-month-old individuals for up to 16 months to three foreshore levels covering the vertical range for this species, representing 20, 50 and 80% of the time spent submerged monthly. Individuals at the upper range limit produced energy more efficiently, as seen by steeper metabolic reactive norms and unaltered ATP levels despite reduced mitochondrial density. By spending most of their time emerged, oysters mounted an antioxidant shielding concomitant with lower levels of pro-oxidant proteins and postponed age-related telomere attrition. Instead, individuals exposed at the lower limit range near subtidal conditions showed lower energy efficiencies, greater oxidative stress and shorter telomere length. These results unraveled the extended acclimatization strategies and the physiological costs of living too fast in subtidal conditions for an intertidal species.

Graphical abstract



Highlights

► Growing at different foreshore levels shape acclimatization in an intertidal shellfish. ► Oysters in high shores produce antioxidant shielding and use energy more efficiently. ► These oysters have longer telomeres than those growing in middle and low shores.

Keywords : Acclimatization, Foreshore, Growth, Metabolism, Oyster, Telomeres

37 **Introduction**

38 Organisms inhabiting variable environments evolved with extended phenotypic plasticity,
39 including acclimatization capacities to endure frequent and intense environmental changes
40 (Burton et al., 2022; Chevin and Hoffmann, 2017; Helmuth et al., 2010). Species within the
41 intertidal zones experience strong variations over short period following daily successions
42 along tide cycles. Intertidal ectotherms are noticeably known for their physiological flexibility
43 to face huge thermal amplitudes and severe changes of their physiology (Clark et al., 2018; L.
44 Li et al., 2018). Emerged individuals should favour maintenance and physiological resistance
45 to multiple constraints when other functions (e.g. growth, storage, reproduction) are
46 hampered. Conversely, regular submersions in sea water near subtidal conditions should keep
47 stimulating aerobic metabolic, physiological processes and possibly accelerate pace of life
48 given that oysters can access and process phytoplankton (Bourlès et al., 2009). Nevertheless,
49 how accelerated growth rates could induce fitness costs in the long run remain to be
50 determined.

51

52 Bivalve molluscs constitute an emblematic clade within intertidal ecosystems (zu Ermgassen
53 et al., 2020). Inter-individual variation in life-history trajectories among conspecifics is
54 greatly explained by geographic gradients. For example, latitudinal changes in temperature
55 explain variation of growth rates and phenology (Fleury et al., 2020; Gourault et al., 2019;
56 Mazaleyrat et al., 2022; Thomas et al., 2016), which are known as major sources of selection
57 in these organisms (L. Li et al., 2018). Such geographic gradients are likely to shape
58 metabolic acclimation to optimise energy use (Gaitán-Espitia et al., 2017). For example in
59 ectotherms, the temperature dependence of metabolic rates may be stronger in cold climates
60 to help individuals performing physiological activities despite suboptimal conditions [e.g.,
61 metabolic cold adaptation, (Dupoué et al., 2017; White et al., 2011)]. Flexible reaction norms

62 may also occur along vertical gradient, across foreshore levels (Dong et al., 2022). Bivalves
63 then represent particularly useful and relevant models to go deeper and explore mechanisms
64 framing contrasted life-history trajectories across foreshore levels.

65

66 Among those, oxidative stress and telomere dynamics have been regularly proposed as the
67 molecular regulators of the pace of life (Andrade et al., 2021; Giraudeau et al., 2019).

68 Oxidative stress arises whenever the natural redox balance is altered due to generation of pro-
69 oxidant compounds [reactive oxygen species (ROS)] that cannot be neutralised by antioxidant
70 activity (Costantini, 2014). ROS are continuously produced by the aerobic metabolism and
71 therefore, individuals with faster pace of life might be more likely to generate oxidative stress
72 (Metcalf and Monaghan, 2001). Enhanced ROS levels can alter the integrity and functions of
73 biomolecules, eventually framing trade-offs between accelerated life style and delayed
74 survival or reproduction costs (Costantini, 2018; Dupoué et al., 2020; Metcalfe and Alonso-
75 Alvarez, 2010). Oxidative stress also contributes to aging by accelerating telomere erosion
76 (Chatelain et al., 2020; Reichert and Stier, 2017). Telomeres, the terminal nucleo-proteins
77 complex capping linear chromosomes, protect DNA from oxidative damages and to help
78 cellular machinery during cell replication (Monaghan et al., 2009). Given that they shorten
79 over cell divisions and may integrate various environmental stresses, they represent relevant
80 biomarkers of long-term and intergenerational fitness costs (Dupoué et al., 2022; Monaghan
81 et al., 2009; Wilbourn et al., 2018). Despite this potential, studies that investigated telomere
82 dynamics in marine ectotherms such as bivalves remain anecdotal (Godwin et al., 2012;
83 Gruber et al., 2014).

84

85 Here, we explored environmental imprinting of metabolic plasticity, oxidative stress markers
86 and telomere dynamics in the intertidal Pacific oyster (*Crassostrea gigas*), a marine bivalve
87 originated from Japan which has spread worldwide due to aquaculture (Troost, 2010).
88 Extensive research on this ecologically and economically important shellfish (i.e., 2 million
89 tons produced each year worldwide) proves an opportunity to clarify cellular and molecular
90 factors implied in response to tide cycle and heat stress (L. Li et al., 2018; Sussarellu et al.,
91 2010; Zhang et al., 2012). This coastal species is relatively competitive in warming sea water
92 due to a hundred copies of gene coding for Heat Shock Protein (HSP) 70 (Zhang et al., 2012).
93 Interestingly, it also possesses a greater number of antioxidant genes as compared to other
94 marine species (Zhang et al., 2016). In Europe, it is now extending its distribution poleward
95 up to Scandinavia (Wrange et al., 2010), but it is facing higher mortality risks at lowest
96 latitudes (Fleury et al., 2020; Mazaleyrat et al., 2022; Pernet et al., 2019). Using the
97 temperature and food dependence of physiological norms (i.e., thermal dependence of
98 physiological processes) in this species, growth rate is forecasted to be a key determinant of
99 oyster persistence in its habitat along latitude (Thomas and Bacher, 2018). The impacts of
100 other environmental gradients, especially bathymetry, should also represent important drivers
101 of contrasted life trajectories (Corporeau et al., 2022; A. Li et al., 2018; Meng et al., 2018). In
102 a previous study, juvenile oysters placed in bags at three foreshore elevations covering
103 intertidal range limits, shaped differential growth rates, resistance to polymicrobial disease
104 and reduction of mortality risks (Corporeau et al., 2022). In the present study, we investigated
105 the molecular and cellular mechanisms of phenotypic responses associated with accelerated
106 life cycles in oysters at the lower foreshore limit compared to those mostly emerged at the
107 upper limit (Fig. 1). We were interested in deciphering the intricate relationships between
108 physiological adjustments (whole organism reaction norms, haemocyte ATP content and
109 mitochondrial density), oxidative stress markers (differential protein expression) and telomere

110 biology (molecular assays). We hypothesized that oysters should acclimatize their physiology
111 to limit thermal dependence of energy expenditure when the oysters grow closed to subtidal
112 habitats. We predict that this lower range limit should expose oysters to greater cellular costs,
113 including oxidative stress and telomere shortening.

114

115 **Material & Methods**

116 *Animals and experimental design*

117 We used diploid *C. gigas* produced by the Ifremer laboratory from standardized gene pools
118 genitors (Fig. 1A, 1B) as extensively detailed in Petton et al. (2015) from three different
119 cohorts (cohort 1: produced in 2017; cohort 2: in 2020; cohort 3: in 2021). Each year (one
120 year corresponds to one cohort, see below), we deployed 2,700 spats (7 months old) in the
121 Bay of Brest (Brittany, France, 48° 20' 06.19" N, 4° 19' 06.37" W) at three foreshore levels,
122 using 3 regular-sized mesh oyster bags per level (triplicates; 300 oysters per bag). This
123 vertical gradient, hereafter called “High” (5m above mean sea level), “Middle” (3m), and
124 “Low” (1.6m) shores differ in time spent submerged over the month, respectively with ca. 20,
125 50, and 80% (Fig. 1C). These three elevations were selected to cover the bathymetric range
126 exploited by this intertidal bivalve in the field. We used thermal probes STPS
127 (<http://www.nke-instrumentation.fr>) to record environmental variation in temperature at 10-
128 min frequency and assess the fluctuating situation of the oysters, either submerged in sea
129 water or emerged in the air. Associated environmental data are available online (Petton et al.,
130 2020).

131

132 We used oysters of cohort 1 (9 months old) to examine short-term physiological responses
133 (proteomic) to different foreshore levels for 2 months while oysters of cohort 2 (17 to 23

134 months old) were studied for ca. 1-year acclimatization responses to contrasted environments
135 (reaction norms of food ingestion and oxygen consumption, mitochondrial density, ATP
136 content, and telomere length). Oysters from cohort 3 (8 months old) were sampled before
137 field deployment and were used as reference for telomere assays (see below). Timing,
138 husbandry conditions, sample size and assays performed on each cohort are summarised in
139 Table S1.

140

141 *Molecular response to foreshore level - Proteomic assays*

142 We collected proteomes in n = 15 oysters (5 individuals per foreshore level), that were flash
143 frozen in liquid nitrogen immediately at collection in the field and stored at -80°C until
144 biochemical assays. Total proteins content was extracted from entire animals following a
145 standard protocol as described previously (Méar et al., 2022) and extensively in
146 Supplementary Information. Briefly, a complete proteome was obtained for each individual
147 using Liquid Chromatography Tandem-Mass Spectrometry (Girard et al., 2022) and
148 alignment of mass spectra on the UniProt KB *C. gigas* protein database (release 31/07/2020;
149 40023 sequences) and a common proteomic contaminant database from the Max Planck
150 Institute of Biochemistry, Martinsried (247 sequences). Functional analysis of protein was
151 performed with topGO R Package using the elim algorithm and a background generated in
152 Ensembl – Biomart (Cunningham et al., 2022) for *C. gigas*, so we could focus our analyses on
153 chaperone proteins and those involved in oxidative stress responses.

154

155 *Cellular responses to foreshore level – Haemocyte energetic efficiency*

156 We collected haemolymphs (ca. 100 µL) in n = 135 oysters of cohort 2 sampled in June 2022
157 at 22 months old to use haemocytes as tools to investigate metabolic alterations at the cellular

158 level. Haemolymph was collected from the pericardiac sinus with an ice-cold 1 ml syringe
159 (non-heparinized) and a 27-gauge needle. Haemocytes were analysed for two indexes of
160 energy production: ATP levels and mitochondrial density. To examine if the food limitation
161 during the acclimation period could interfere with the results, half animals were fed *ad libitum*
162 with *Tisochrysis lutea* while the other half were kept fasted a week before sampling. We used
163 colorimetric assays to determine ATP content in haemolymph freshly sampled (CellTiter
164 GLO®, PROMEGA G7570) and mitochondrial density from haemolymph fixed in
165 formaldehyde (MITO-ID®, Enzo Life Science). Samples were measured in duplicates
166 following a protocol detailed in Supplementary Information.

167

168 *Cellular response to foreshore level - Telomere assays*

169 Multiple tests were performed to optimise a protocol for telomere assay in oysters from the
170 cohorts 2 sampled in June 2022 at 22 months old (i.e., 15 months in the field) and cohort 3
171 sampled in May 2022 at 8 months old. DNA was extracted using DNA Isolation kit for cell
172 and tissue (Sigma Aldrich, Roche) from 20-30 mg oyster gills freshly sampled. We sampled
173 gills because this tissue has been previously used in the few telomere studies on bivalves
174 (Godwin et al., 2012; Gruber et al., 2014). We used a NanoDrop 2000 (Thermo Scientific) to
175 check that absorbance ratios of extracted DNA met the optimal criteria (mean \pm SD,
176 A260/A280: 1.88 ± 0.05 , A260/A230: 2.22 ± 0.30). As detailed in Supplementary
177 Information, we also performed gel electrophoresis to confirm the purification of high
178 molecular weight DNA. Then, we used two methods to quantify telomere length (TL) using
179 absolute (Telomere Restriction Fragment - TRF) and relative quantifications (quantitative
180 Polymerase Chain Reaction - qPCR). TRF method is based on an initial DNA digestion with
181 two restriction enzymes (*Hinf I* and *Rsa I*), followed by a gel electrophoresis for 4h (0.8%
182 agarose) and southern blot technics from the TeloTTAGG assay kit (Sigma Aldrich, Roche).

183 We followed the protocol described by the manufacturer to obtain absolute TL measures from
184 n = 10 oysters of cohort 3. We used these 8 month old individuals (range of TL: 5.06 - 9.36
185 kb) to control that TL provided reliable estimates regardless of the methods. qPCR protocol
186 for telomere assay was performed on a thermocycler using *Sybr Green Supermix* (BioRad,
187 California, USA) and optimised from the protocol proposed by (Cawthon, 2009) as detailed in
188 supplementary methods. Samples were measured in triplicates and each run included a pool of
189 DNA as a gold standard and blank control (water) for each primer pair. Samples relative
190 quantification values were normalized to a unique copy gene in *C. gigas* genome (GAPDH)
191 and relative to the gold standard as recommended by Pfaffl (2001) to measure relative
192 telomere length (rTL) as follow:

$$193 \text{ rTL} = \frac{2.016^{(Cq \text{ telomere}_{Pool} - Cq \text{ telomere}_{Sample})}}{2.071^{(Cq \text{ GAPDH}_{Pool} - Cq \text{ GAPDH}_{Sample})}}$$

194

195 *Whole organism response to foreshore level - Thermal reaction norms*

196 We assayed thermal reaction norms in n = 60 individuals from cohort 2 sampled in January
197 2022 at 17 months old (i.e., 10 months in the field), and maintained in laboratory at ca. 12°C
198 without food until being assayed. Oysters were acclimated in a 300 L tank with seawater
199 running at 300 L/h. We used a COSA system to determine the temperature-dependence of
200 oxygen consumption (VO_2) as index of aerobic maximal metabolic rate (MMR) and filtration
201 rates at four temperature: 13, 19, 25 and 31°C, a thermal range covering temperature naturally
202 experienced by oysters in the field (13 to 25°C) and one closed to high-temperature limit
203 (31°C). As previously explained (Pousse et al., 2018; Tallec et al., 2021) and detailed in
204 Supplementary Information, this multiplexed system allows to automatically switch between
205 9 chambers (8 occupied by individuals, 1 left empty as reference). Water temperature was
206 controlled upstream within four-water tanks using 300W resistances and thermostats and

207 circulated in the system using two peristaltic pumps. We designed a program to automatically
208 switch between chambers every 8 min using solenoid valves. Water of the selected chamber
209 was analysed downstream by an oxygen optical sensor (WTW Multi 3430, O₂ ± 0.05 mg/L), a
210 fluorometer (WetLabs, SeaBird, USA, Fluorometry ± 0.1 FFU), a flow meter (Sonoflow,
211 Sonotec GmbH; FR ± 0.1 ml/sec), and a pH meter (WTW Multi 3430, pH ± 0.05 NBS scale).
212 We considered the flow rate (mean ± SD: 28.3 ± 2.8 ml/min) and the differential in
213 fluorometric signals (in FFU) or O₂ concentration (mg/ml) between the reference chamber
214 and each animal chambers to determine filtration rate and VO₂. We obtained individual
215 reaction norms for both filtration rate and MMR. Fitting the Arrhenius curve from oysters
216 reactive norms of MMR, the Arrhenius temperature T_A represents the slope of the
217 temperature-metabolic relationship, and provides an individual estimation of energy
218 activation and thermal dependence in metabolic rate (Kooijman, 2010):

$$219 \quad k(T) = k_1 \cdot e^{\frac{T_A}{T_1} - \frac{T_A}{T}}$$

220 T_A was obtained for each oyster, where k is the mean VO₂ measure at a given temperature T ,
221 from a reference rate (k_1 , here estimated at a reference temperature $T_1 = 25^\circ\text{C}$).

222

223 *Statistical analyses*

224 Molecular responses to foreshore level (differential protein expression) were analysed using
225 the R package BetaBinomial 1.2 implemented in Proline Studio 2.0.1. We compiled proteins
226 of interest (chaperone proteins and those involved in response to oxidative stress) identified
227 with differential expression between foreshore levels (significant enrichment was set using an
228 exact Fisher test p-value < 0.05) within R software [R Core Team (2021)] in a Principal
229 Component Analysis [package ade4 (Dray and Dufour, 2007)] to ease visualization of
230 multivariate proteomic profiles.

231

232 Cellular and physiological responses to foreshore levels were analysed with linear models and
233 linear mixed models [package *nlme* (Pinheiro et al., 2020)]. For all tested variables, we built a
234 complete model, including all possible fixed factors and their interaction, and we used the
235 *dredge* function to compare and rank all model performance, based on AICc (see Table S2)
236 [package *MuMIn* (Barton, 2019)]. We thus identified the fixed terms of interest without *a*
237 *priori* expectations. Oyster weight (shell and flesh) was primarily influenced by foreshore
238 level due to strong differences in growth rates (Corporeau et al., 2022) so we scaled body
239 weight (log transformed) within each foreshore level [package *standardize* (Eager, 2017)] to
240 control for allometry while limiting collinearity among explanatory factors. ATP production
241 and mitochondrial density were analysed with linear models, testing the effects of body
242 weight (log transformed), food access (fed or unfed), foreshore level and first order
243 interaction terms. We analysed factors explaining variations in TL using two independent
244 model sets. First, we examined the effect of age, comparing TL in oysters from cohort 3 (8-
245 month old) to those from cohort 2 (22-month old). Second, in 22-month old oysters, we built
246 a separate model to investigate the effects of body weight (log transformed), foreshore level
247 and first order interaction. Thermal reaction norms were measured on the same animals at the
248 4 temperatures so we set oyster identity as random intercept. Filtration rate and VO_2 (log
249 transformed) were treated as dependent variables and we tested the fixed effects of scaled
250 body weight, number of days fasted, linear and quadratic effect of temperature, foreshore
251 level and first order interaction.

252

253 We determined quality of cellular and physiological assays by checking repeatability among
254 samples and individuals using rptR package (Stoffel et al., 2017).

255

256 **Results**

257 *Molecular responses to foreshore levels*

258 After two months in the field, foreshore level shaped differential expression of multiple
259 proteomic markers of response to thermal stress and antioxidant defenses in High shore (all B
260 Binomial tests ; $p < 0.05$). Oysters from this upper shore limits exhibited greater production of
261 HSP 70 together with multiple antioxidant proteins, including the superoxide dismutase, 3
262 catalases, peroxidase YfeX, peroxiredoxin, non-selenium glutathione peroxidase and a
263 peptide-methionine (R)-S-oxide reductase compared to oysters from Middle and Low shores
264 (Fig. 2). On the contrary, oysters from Low shores showed higher HSP 90 and glutathione
265 peroxidase (Fig. 2). These oysters regularly submerged also experienced higher risk of
266 oxidative attacks by two NADPH oxidase (Fig. 2).

267

268 *Cellular responses to foreshore level*

269 Haemocyte energetic efficiency

270 ATP content and mitochondrial density showed high repeatability (respectively $r = 0.99$, $p <$
271 0.001 and $r = 0.92$, $p < 0.001$). ATP content did not differ between foreshore levels and was
272 only influenced by food access (fed oysters showed higher ATP content than fasted ones)
273 (Fig. 3A). Conversely, variation in mitochondrial density significantly differed between
274 foreshore levels, being lower in High compared to Middle and Low shore oysters (Table 1,
275 Table S2, Fig. 3B).

276

277 Telomere dynamics

278 Assays of individual rTL showed good repeatability among plates ($r = 0.76$, $p < 0.001$). RTL
279 decreases with age (Table 1, Table S2, Fig. 4). In addition, at 22-month old, rTL was
280 influenced by foreshore level irrespective of the interaction term (Table S2). Oysters from
281 High shores exhibited 28% longer rTL compared to Middle and Low shore individuals (Table
282 1, Fig. 4).

283

284 *Physiological acclimatization at whole organism level*

285 Filtration rate was positively influenced by oyster weight (range: 1.5 - 21.2 g), number of
286 days spent starved (range: 5 - 27 days), linear and quadratic slope along temperature and
287 foreshore level (Table 1, Table S2). Filtration was highly variable, even within individuals (r
288 $= 0.38$, $p < 0.001$) but on average, filtration rates noticeably dropped at high temperature
289 irrespective of foreshore level (Fig. 5A), and significantly more for Low shores oysters
290 (interaction term, Table 1, Fig. 5A). Maximum metabolic rate was more repeatable within
291 individuals ($r = 0.91$, $p < 0.001$) and positively influenced by oyster weight, linear slope with
292 temperature, and first order interaction term between foreshore level and temperature (Table
293 1, Table S2). Metabolic reaction norm was steeper in individuals from High compared to Low
294 shore level, while Middle ones were intermediate (Table 1, Fig. 5B). On average, this resulted
295 in Arrhenius temperatures greater in High shore oysters ($T_A = 8968 \pm 323K$) compared to
296 Middle ($T_A = 7685 \pm 431K$, $t = -2.3$, $p = 0.023$) and Low ones ($T_A = 7017 \pm 445K$, $t = -3.5$, p
297 $= 0.001$).

298

299 **Discussion**

300 In this study, we investigated the physiological determinants of phenotypic plasticity in the
301 Pacific oyster along a vertical gradient of bathymetry. In line with previous examinations

302 highlighting contrasted life history trade-off between growth rates and mortality risk
303 (Corporeau et al., 2022), we found that foreshore level shaped differential life trajectories
304 sustained by physiological acclimatization. That is, oysters exposed to aerial conditions most
305 part of their life mounted an antioxidant shielding and experience slower growth rate. These
306 oysters also gained in metabolic efficiencies given that they appeared more efficient to
307 produce energy (steeper metabolic reaction norms and ATP concentration) despite lower
308 mitochondrial density. In the opposite range limits, at Low intertidal levels, oysters grew
309 faster at the cost of faster telomere attrition, suggesting acceleration of the aging rate. Below,
310 we discussed these results and their implications in explaining vertical range limits.

311

312 A first sign of short-term acclimatization to different foreshore levels, oysters modified their
313 proteomes related to thermal stress avoidance and oxidative stress responses after two months.
314 Proteomic profiles differed between intertidal conditions, as shown by the over-expression of
315 chaperone and antioxidant proteins in oysters that endure regular emersion. For instance, we
316 observed higher levels of HSP 70 concomitantly with adaptations of intertidal organisms to
317 limit the risk of frequent heat stress in High shores (A. Li et al., 2018; Wang et al., 2021).
318 Instead, oysters from Low shores experienced greater HSP 90 and glutathione peroxidase
319 levels, which may respond to metabolic activities in subtidal conditions. In this environment,
320 oysters may experience greater ROS production, given that they showed higher levels of
321 NADPH oxidase (Dupuy et al., 1991). In addition poorer neutralization by lower level of
322 endogenous antioxidant may exacerbate oxidative stress in oysters submerged most of their
323 time, which could ultimately trade faster growth rate against survival (Buttemer et al., 2010).
324 Instead, in oysters within High shores experiencing regular hypoxia during low tide (i.e., less
325 ROS production), it remains uncertain why they also mounted an antioxidant shielding. As
326 previously hypothesized, intertidal bivalves may boost production of endogenous antioxidant

327 during low tides in anticipation of the metabolic burst during the next submersion (Almeida
328 and Bainy, 2006; Andrade et al., 2021; Sussarellu et al., 2010). In support of this statement,
329 we also found that High shore oysters were those with enhanced metabolic reaction norm as
330 discussed hereafter.

331

332 Individuals further showed significant adjustments of energy metabolism after 4 more months
333 in different habitats. Temperature dependence of physiological rates appeared significantly
334 impacted by foreshore levels, including steeper reaction norms of filtration and maximal
335 metabolic rates in High shore oysters. These whole-organism responses provide reliable
336 measures acclimatization, in line with previous evidences that ectotherms may optimize the
337 limits imposed by fewer opportunities to initiate physiological rates by upregulating thermal
338 dependence of metabolism (Dupoué et al., 2017; White et al., 2011). In other words, oysters
339 from High shores probably showed steeper metabolic reaction norms to optimize
340 physiological processes despite fewer opportunities to generate and mobilize energy (only
341 20% of time spent submerged). This is allowed by Arrhenius temperature (inversely
342 proportional to energy activation) ca. 20% greater in High shore oysters compared to Middle
343 and Low shore levels. Growing 9 months at contrasted foreshore level, oysters also
344 experienced similar energy content and thus, despite lower mitochondrial density. Previous
345 microscopic examinations have highlighted that ultrastructure of mitochondria is modified by
346 foreshore level as a result of a metabolic reprogramming in harsh intertidal environments
347 (Corporeau et al., 2022). Altogether, these results at cellular and individual levels suggest that
348 growing in High shore elevations more efficiently generate energy. A differential in
349 mitochondrial efficiencies would imply greater ratio ATP/O (Metcalf and Olsson, 2022),
350 which we hypothesize to be optimized in High shore oysters. Further investigations using *in*
351 *situ* assays (e.g., high-resolution respirometry, mitochondrial bioenergetics, and

352 metabolomics) will allow us to explore how foreshore level may reshape mitochondrial
353 functioning.

354

355 Eventually, acclimatizing to foreshore level had further consequences on telomere dynamics.
356 Telomere length decreases with age as regularly documented in other animals (Dunshea et al.,
357 2011), however the age-related telomere erosion additionally depended upon environment
358 conditions. That is, telomeres were shorter in oysters from Middle and Low shores compared
359 to those from High shores. This result suggests that living faster may come at the cost of
360 accelerated aging pace when a species adapted to intertidal habitats approach distribution
361 range limits closed to subtidal conditions. It is worth noting that individual rTL was not
362 correlated to oyster weight (flesh and shell), implying that telomere may not erode as direct
363 consequence of growth rate. Our results rather suggest that telomeres shorten as consequence
364 of enhanced oxidative stress, related to subtidal conditions, as in other species (Chatelain et
365 al., 2020; Reichert and Stier, 2017). Another functional explanation may involve DNA
366 hypermethylation in subtidal environments (Clark et al., 2018; Wang et al., 2021), which
367 might in turn alter telomere dynamics (Sheldon et al., 2021). Further evidence is now needed
368 to i) identify the most relevant environmental factors shaping telomere erosion (e.g., sea
369 surface temperature, food quantity and/or quality), ii) quantify the degree of telomere
370 heritability, iii) explore the role of telomere length in shaping fitness costs (mortality risks,
371 lifespan, reproductive investment and success), and iv) establish a model of environment-
372 telomere-lifespan [e.g., Weibull acceleration ageing factors; (Kooijman, 2010)]. This will
373 allow using this species as a model to understand altered aging pace when facing global
374 changes.

375

376 **Conclusion**

377 Phenotypic plasticity is essential to thrive when exposed to rapid environmental variation, and
378 it will constitute a critical determinant of species persistence toward ongoing global changes
379 (Somero, 2010). As reported here and in line with many studies, we confirmed the extreme
380 plasticity of the intertidal Pacific oyster. Despite being originated from a standardized genetic
381 pool, foreshore level strongly imprinted life trajectories through variable growth rates. It
382 remains to clarify whether acclimatization to foreshore level would persist in time or if it is
383 reversible after few months. Then, bringing oysters back to common garden conditions (e.g.,
384 same foreshore level) for a year should help to decipher between phenotypic flexibility and/or
385 developmental plasticity in this intertidal bivalve. In addition, this study probably reflects at
386 what costs plasticity arises, as unraveled by greater oxidative stress and aging pace when
387 growing faster even though oysters downregulated temperature dependence of metabolic
388 rates. In support of high flexibility, *C. gigas* is now colonizing elevated latitudes, thanks to
389 warming ocean, where summer temperature allows reproductive events (Thomas et al., 2016).
390 Conversely, this species survive less in its southern limit range, where it is enduring mass
391 mortality events (Fleury et al., 2020). Eventually, bathymetry might select genotypes resistant
392 to subtidal conditions (Meng et al., 2018). We hypothesize that altered telomere dynamics
393 could constitute one of the central tenet of natural (expansion) or artificial (farming) selection.
394 If telomere triggers fitness costs, as in most species, we predict that this cellular marker
395 should explain foreshore range limits bearable for intertidal ectotherms.

396

397 **References**

- 398 Almeida, E.A., Bainy, A.C.D., 2006. Effects of Aerial Exposure on Antioxidant Defenses in the Brown
399 Mussel *Perna perna*. *Braz. Arch. Biol. Technol.* 49, 225–229.
400 Andrade, M., Rivera-Ingraham, G., Soares, A.M.V.M., Miranda Rocha, R.J., Pereira, E., Solé, M.,
401 Freitas, R., 2021. How do life-history traits influence the fate of intertidal and subtidal *Mytilus*

402 *galloprovincialis* in a changing climate? Environ. Res. 196, 110381.
403 <https://doi.org/10.1016/j.envres.2020.110381>

404 Barton, K., 2019. MuMIn: Multi-Model Inference. R Package Version 1436.

405 Bourlès, Y., Alunno-Bruscia, M., Pouvreau, S., Tollu, G., Leguay, D., Arnaud, C., Gouletquer, P.,
406 Kooijman, S.A.L.M., 2009. Modelling growth and reproduction of the Pacific oyster
407 *Crassostrea gigas*: Advances in the oyster-DEB model through application to a coastal pond.
408 J. Sea Res. 62, 62–71. <https://doi.org/10.1016/j.seares.2009.03.002>

409 Burton, T., Ratikainen, I.I., Einum, S., 2022. Environmental change and the rate of phenotypic
410 plasticity. Glob. Change Biol. 28, 5337–5345. <https://doi.org/10.1111/gcb.16291>

411 Buttemer, W.A., Abele, D., Costantini, D., 2010. From bivalves to birds: Oxidative stress and longevity.
412 Funct. Ecol. 24, 971–983. <https://doi.org/10.1111/j.1365-2435.2010.01740.x>

413 Cawthon, R.M., 2009. Telomere length measurement by a novel monochrome multiplex quantitative
414 PCR method. Nucleic Acids Res. 37, e21. <https://doi.org/10.1093/nar/gkn1027>

415 Chatelain, M., Drobniak, S.M., Szulkin, M., 2020. The association between stressors and telomeres in
416 non-human vertebrates: a meta-analysis. Ecol. Lett. 23, 381–398.
417 <https://doi.org/10.1111/ele.13426>

418 Chevin, L.-M., Hoffmann, A.A., 2017. Evolution of phenotypic plasticity in extreme environments.
419 Philos. Trans. R. Soc. B Biol. Sci. 372, 20160138. <https://doi.org/10.1098/rstb.2016.0138>

420 Clark, M.S., Thorne, M.A.S., King, M., Hipperson, H., Hoffman, J.I., Peck, L.S., 2018. Life in the
421 intertidal: Cellular responses, methylation and epigenetics. Funct. Ecol. 32, 1982–1994.
422 <https://doi.org/10.1111/1365-2435.13077>

423 Corporeau, C., Petton, S., Vilaça, R., Delisle, L., Quéré, C., Le Roy, V., Dubreuil, C., Lacas-Gervais, S.,
424 Guitton, Y., Artigaud, S., Bernay, B., Pichereau, V., Huvet, A., Petton, B., Pernet, F., Fleury, E.,
425 Madec, S., Brigaudeau, C., Brenner, C., Mazure, N.M., 2022. Harsh intertidal environment
426 enhances metabolism and immunity in oyster (*Crassostrea gigas*) spat. Mar. Environ. Res.
427 180, 105709. <https://doi.org/10.1016/j.marenvres.2022.105709>

428 Costantini, D., 2018. Meta-analysis reveals that reproductive strategies are associated with sexual
429 differences in oxidative balance across vertebrates. Curr. Zool. 64, 1–11.
430 <https://doi.org/10.1093/cz/zox002>

431 Costantini, D., 2014. Oxidative Stress and Hormesis in Evolutionary Ecology and Physiology, Oxidative
432 Stress and Hormesis in Evolutionary Ecology and Physiology. <https://doi.org/10.1007/978-3-642-54663-1>

434 Cunningham, F., Allen, J.E., Allen, J., Alvarez-Jarreta, J., Amode, M.R., Armean, I.M., Austine-
435 Orimoloye, O., Azov, A.G., Barnes, I., Bennett, R., Berry, A., Bhai, J., Bignell, A., Billis, K.,
436 Boddu, S., Brooks, L., Charkhchi, M., Cummins, C., Da Rin Fioretto, L., Davidson, C., Dodiya, K.,
437 Donaldson, S., El Houdaigui, B., El Naboulsi, T., Fatima, R., Giron, C.G., Genez, T., Martinez,
438 J.G., Guijarro-Clarke, C., Gymer, A., Hardy, M., Hollis, Z., Hourlier, T., Hunt, T., Juettemann, T.,
439 Kaikala, V., Kay, M., Lavidas, I., Le, T., Lemos, D., Marugán, J.C., Mohanan, S., Mushtaq, A.,
440 Naven, M., Ogeh, D.N., Parker, A., Parton, A., Perry, M., Piližota, I., Prosovetskaia, I.,
441 Sakthivel, M.P., Salam, A.I.A., Schmitt, B.M., Schuilenburg, H., Sheppard, D., Pérez-Silva, J.G.,
442 Stark, W., Steed, E., Sutinen, K., Sukumaran, R., Sumathipala, D., Suner, M.-M., Szpak, M.,
443 Thormann, A., Tricomi, F.F., Urbina-Gómez, D., Veidenberg, A., Walsh, T.A., Walts, B.,
444 Willhoft, N., Winterbottom, A., Wass, E., Chakiachvili, M., Flint, B., Frankish, A., Giorgetti, S.,
445 Haggerty, L., Hunt, S.E., Ilsley, G.R., Loveland, J.E., Martin, F.J., Moore, B., Mudge, J.M.,
446 Muffato, M., Perry, E., Ruffier, M., Tate, J., Thybert, D., Trevanion, S.J., Dyer, S., Harrison,
447 P.W., Howe, K.L., Yates, A.D., Zerbino, D.R., Flicek, P., 2022. Ensembl 2022. Nucleic Acids Res.
448 50, D988–D995. <https://doi.org/10.1093/nar/gkab1049>

449 Dong, Y., Liao, M., Han, G., Somero, G.N., 2022. An integrated, multi-level analysis of thermal effects
450 on intertidal molluscs for understanding species distribution patterns. Biol. Rev. 97, 554–581.
451 <https://doi.org/10.1111/brv.12811>

452 Dray, S., Dufour, A.B., 2007. The ade4 package: implementing the duality diagram for ecologists. J.
453 Stat. Softw. 22, 1–20.

454 Dunshea, G., Duffield, D., Gales, N., Hindell, M., Wells, R.S., Jarman, S.N., 2011. Telomeres as age
455 markers in vertebrate molecular ecology. *Mol. Ecol.* 11, 225–235.
456 <https://doi.org/10.1111/j.1755-0998.2010.02976.x>

457 Dupoué, A., Blaimont, P., Angelier, F., Ribout, C., Rozen-Rechels, D., Richard, M., Miles, D., de
458 Villemereuil, P., Rutschmann, A., Badiane, A., Aubret, F., Lourdais, O., Meylan, S., Cote, J.,
459 Clobert, J., Le Galliard, J.-F., 2022. Lizards from warm and declining populations are born with
460 extremely short telomeres. *Proc. Natl. Acad. Sci.* 119, e2201371119.
461 <https://doi.org/10.1073/pnas.2201371119>

462 Dupoué, A., Blaimont, P., Rozen-Rechels, D., Richard, M., Meylan, S., Clobert, J., Miles, D.B., Martin,
463 R., Decencièrre, B., Agostini, S., Le Galliard, J.-F., 2020. Water availability and temperature
464 induce changes in oxidative status during pregnancy in a viviparous lizard. *Funct. Ecol.* 34,
465 475–485. <https://doi.org/10.1111/1365-2435.13481>

466 Dupoué, A., Brischoux, F., Lourdais, O., 2017. Climate and foraging mode explain interspecific
467 variation in snake metabolic rates. *Proc. R. Soc. B Biol. Sci.* 284, 20172108–20172108.

468 Dupuy, C., Virion, A., Ohayon, R., Kaniewski, J., Dème, D., Pommier, J., 1991. Mechanism of hydrogen
469 peroxide formation catalyzed by NADPH oxidase in thyroid plasma membrane. *J. Biol. Chem.*
470 266, 3739–3743. [https://doi.org/10.1016/S0021-9258\(19\)67857-9](https://doi.org/10.1016/S0021-9258(19)67857-9)

471 Eager, C.D., 2017. standardize: Tools for Standardizing Variables for Regression in R.

472 Fleury, E., Barbier, P., Petton, B., Normand, J., Thomas, Y., Pouvreau, S., Daigle, G., Pernet, F., 2020.
473 Latitudinal drivers of oyster mortality: deciphering host, pathogen and environmental risk
474 factors. *Sci. Rep.* 10, 7264. <https://doi.org/10.1038/s41598-020-64086-1>

475 Gaitán-Espitia, J.D., Bacigalupe, L.D., Opitz, T., Lagos, N.A., Osoreo, S., Lardies, M.A., 2017. Exploring
476 physiological plasticity and local thermal adaptation in an intertidal crab along a latitudinal
477 cline. *J. Therm. Biol.* 68, 14–20. <https://doi.org/10.1016/j.jtherbio.2017.02.011>

478 Girard, O., Lavigne, R., Chevolleau, S., Onfray, C., Com, E., Schmit, P.-O., Chapelle, M., Fréour, T.,
479 Lane, L., David, L., Pineau, C., 2022. Naive Pluripotent and Trophoblastic Stem Cell Lines as a
480 Model for Detecting Missing Proteins in the Context of the Chromosome-Centric Human
481 Proteome Project. *J. Proteome Res.* *acs.jproteome.2c00496*.
482 <https://doi.org/10.1021/acs.jproteome.2c00496>

483 Giraudeau, M., Angelier, F., Sepp, T., 2019. Do Telomeres Influence Pace-of-Life-Strategies in
484 Response to Environmental Conditions Over a Lifetime and Between Generations? *BioEssays*
485 41, 1800162. <https://doi.org/10.1002/bies.201800162>

486 Godwin, R., Brown, I., Montgomery, S., Frusher, S., Green, T., Ovenden, J., 2012. Telomere dynamics
487 in the Sydney rock oyster (*Saccostrea glomerata*): an investigation into the effects of age,
488 tissue type, location and time of sampling. *Mar. Biol.* 159, 77–86.
489 <https://doi.org/10.1007/s00227-011-1791-7>

490 Gourault, M., Petton, S., Thomas, Y., Pecquerie, L., Marques, G.M., Cassou, C., Fleury, E., Paulet, Y.M.,
491 Pouvreau, S., 2019. Modeling reproductive traits of an invasive bivalve species under
492 contrasting climate scenarios from 1960 to 2100. *J. Sea Res.* 143, 128–139.
493 <https://doi.org/10.1016/j.seares.2018.05.005>

494 Gruber, H., Schaible, R., Ridgway, I.D., Chow, T.T., Held, C., Philipp, E.E.R., 2014. Telomere-
495 independent ageing in the longest-lived non-colonial animal, *Arctica islandica*. *Exp. Gerontol.*
496 51, 38–45. <https://doi.org/10.1016/j.exger.2013.12.014>

497 Helmuth, B., Broitman, B.R., Yamane, L., Gilman, S.E., Mach, K., Mislán, K.A.S., Denny, M.W., 2010.
498 Organismal climatology: analyzing environmental variability at scales relevant to
499 physiological stress. *J. Exp. Biol.* 213, 995–1003. <https://doi.org/10.1242/jeb.038463>

500 Kooijman, S.A.L.M., 2010. Dynamic energy budget theory for metabolic organisation, *Dynamic Energy*
501 *Budget Theory for Metabolic Organisation*, Third Edition. Cambridge University Press.
502 <https://doi.org/10.1017/CBO9780511805400>

503 Li, A., Li, L., Wang, W., Song, K., Zhang, G., 2018. Transcriptomics and Fitness Data Reveal Adaptive
504 Plasticity of Thermal Tolerance in Oysters Inhabiting Different Tidal Zones. *Front. Physiol.* 9,
505 825. <https://doi.org/10.3389/fphys.2018.00825>

506 Li, L., Li, A., Song, K., Meng, J., Guo, X., Li, S., Li, C., De Wit, P., Que, H., Wu, F., Wang, W., Qi, H., Xu, F.,
507 Cong, R., Huang, B., Li, Y., Wang, T., Tang, X., Liu, S., Li, B., Shi, R., Liu, Y., Bu, C., Zhang, C., He,
508 W., Zhao, S., Li, H., Zhang, S., Zhang, L., Zhang, G., 2018. Divergence and plasticity shape
509 adaptive potential of the Pacific oyster. *Nat. Ecol. Evol.* 2, 1751–1760.
510 <https://doi.org/10.1038/s41559-018-0668-2>

511 Mazaleyrat, A., Normand, J., Dubroca, L., Fleury, E., 2022. A 26-year time series of mortality and
512 growth of the Pacific oyster *C. gigas* recorded along French coasts. *Sci. Data* 9, 392.
513 <https://doi.org/10.1038/s41597-022-01511-2>

514 Méar, L., Com, E., Fathallah, K., Guillot, L., Lavigne, R., Guével, B., Fauconnier, A., Vialard, F., Pineau,
515 C., 2022. The Eutopic Endometrium Proteome in Endometriosis Reveals Candidate Markers
516 and Molecular Mechanisms of Physiopathology. *Diagnostics* 12, 419.
517 <https://doi.org/10.3390/diagnostics12020419>

518 Meng, J., Wang, T., Li, L., Zhang, G., 2018. Inducible variation in anaerobic energy metabolism reflects
519 hypoxia tolerance across the intertidal and subtidal distribution of the Pacific oyster
520 (*Crassostrea gigas*). *Mar. Environ. Res.* 138, 135–143.
521 <https://doi.org/10.1016/j.marenvres.2018.04.002>

522 Metcalfe, N.B., Alonso-Alvarez, C., 2010. Oxidative stress as a life-history constraint: The role of
523 reactive oxygen species in shaping phenotypes from conception to death. *Funct. Ecol.* 24,
524 984–996. <https://doi.org/10.1111/j.1365-2435.2010.01750.x>

525 Metcalfe, N.B., Monaghan, P., 2001. Compensation for a bad start: Grow now, pay later? *Trends Ecol.*
526 *Evol.* 16, 254–260. [https://doi.org/10.1016/S0169-5347\(01\)02124-3](https://doi.org/10.1016/S0169-5347(01)02124-3)

527 Metcalfe, N.B., Olsson, M., 2022. How telomere dynamics are influenced by the balance between
528 mitochondrial efficiency, reactive oxygen species production and DNA damage. *Mol. Ecol.* 31,
529 6040–6052. <https://doi.org/10.1111/mec.16150>

530 Monaghan, P., Metcalfe, N.B., Torres, R., 2009. Oxidative stress as a mediator of life history trade-
531 offs: mechanisms, measurements and interpretation. *Ecol. Lett.* 12, 75–92.
532 <https://doi.org/10.1111/j.1461-0248.2008.01258.x>

533 Pernet, F., Gachelin, S., Stanisière, J.Y., Petton, B., Fleury, E., Mazurié, J., Byron, C., 2019. Farmer
534 monitoring reveals the effect of tidal height on mortality risk of oysters during a herpesvirus
535 outbreak. *ICES J. Mar. Sci.* 76, 1816–1824. <https://doi.org/10.1093/icesjms/fsz074>

536 Petton, B., Boudry, P., Alunno-Bruscia, M., Pernet, F., 2015. Factors influencing disease-induced
537 mortality of Pacific oysters *Crassostrea gigas*. *Aquac. Environ. Interact.* 6, 205–222.
538 <https://doi.org/10.3354/aei00125>

539 Petton, S., Corporeau, C., Quemener, L., 2020. Temperature Monitoring of Subtidal and Intertidal
540 Microhabitats of Oyster *Crassostrea gigas*. *SEANOE Data Set*. <https://doi.org/10.17882/79095>

541 Pinheiro, J., Bates, D., DebRoy, S., Sarkar, D., R, C.T., 2020. nlme: Linear and Nonlinear Mixed Effects
542 Models.

543 Pousse, É., Flye-Sainte-Marie, J., Alunno-Bruscia, M., Hégaret, H., Jean, F., 2018. Sources of paralytic
544 shellfish toxin accumulation variability in the Pacific oyster *Crassostrea gigas*. *Toxicon* 144,
545 14–22. <https://doi.org/10.1016/j.toxicon.2017.12.050>

546 Reichert, S., Stier, A., 2017. Does oxidative stress shorten telomeres in vivo? A review. *Biol. Lett.*

547 Sheldon, E.L., Ton, R., Boner, W., Monaghan, P., Raveh, S., Schrey, A.W., Griffith, S.C., 2021.
548 Associations between DNA methylation and telomere length during early life: Insight from
549 wild zebra finches (*Taeniopygia guttata*). *Mol. Ecol. mec.* 16187.
550 <https://doi.org/10.1111/mec.16187>

551 Somero, G.N., 2010. The physiology of climate change: how potentials for acclimatization and genetic
552 adaptation will determine “winners” and “losers.” *J. Exp. Biol.* 213, 912–920.
553 <https://doi.org/10.1242/jeb.037473>

554 Stoffel, M.A., Nakagawa, S., Schielzeth, H., 2017. rptR: repeatability estimation and variance
555 decomposition by generalized linear mixed-effects models. *Methods Ecol. Evol.* 8, 1639–
556 1644. <https://doi.org/10.1111/2041-210X.12797>

558 Sussarellu, R., Fabioux, C., Le Moullac, G., Fleury, E., Moraga, D., 2010. Transcriptomic response of
559 the Pacific oyster *Crassostrea gigas* to hypoxia. *Mar. Genomics* 3, 133–143.
560 <https://doi.org/10.1016/j.margen.2010.08.005>

561 Tallec, K., Paul-Pont, I., Petton, B., Alunno-Bruscia, M., Bourdon, C., Bernardini, I., Boulais, M.,
562 Lambert, C., Quéré, C., Bideau, A., Le Goïc, N., Cassone, A.-L., Le Grand, F., Fabioux, C.,
563 Soudant, P., Huvet, A., 2021. Amino-nanopolystyrene exposures of oyster (*Crassostrea gigas*)
564 embryos induced no apparent intergenerational effects. *Nanotoxicology* 1–17.
565 <https://doi.org/10.1080/17435390.2021.1879963>

566 Thomas, Y., Bacher, C., 2018. Assessing the sensitivity of bivalve populations to global warming using
567 an individual-based modelling approach. *Glob. Change Biol.* 24, 4581–4597.
568 <https://doi.org/10.1111/gcb.14402>

569 Thomas, Y., Pouvreau, S., Alunno-Bruscia, M., Barillé, L., Gohin, F., Bryère, P., Gernez, P., 2016. Global
570 change and climate-driven invasion of the Pacific oyster (*Crassostrea gigas*) along European
571 coasts: a bioenergetics modelling approach. *J. Biogeogr.* 43, 568–579.
572 <https://doi.org/10.1111/jbi.12665>

573 Troost, K., 2010. Causes and effects of a highly successful marine invasion: Case-study of the
574 introduced Pacific oyster *Crassostrea gigas* in continental NW European estuaries. *J. Sea Res.*
575 64, 145–165. <https://doi.org/10.1016/j.seares.2010.02.004>

576 Wang, X., Li, A., Wang, W., Que, H., Zhang, G., Li, L., 2021. DNA methylation mediates differentiation
577 in thermal responses of Pacific oyster (*Crassostrea gigas*) derived from different tidal levels.
578 *Heredity* 126, 10–22. <https://doi.org/10.1038/s41437-020-0351-7>

579 White, C.R., Alton, L.A., Frappell, P.B., 2011. Metabolic cold adaptation in fishes occurs at the level of
580 whole animal, mitochondria and enzyme. *Proc. R. Soc. B Biol. Sci.* 279, 1740–1747.
581 <https://doi.org/10.1098/rspb.2011.2060>

582 Wilbourn, R.V., Moatt, J.P., Froy, H., Walling, C.A., Nussey, D.H., Boonekamp, J.J., 2018. The
583 relationship between telomere length and mortality risk in non-model vertebrate systems: a
584 meta-analysis. *Philos. Trans. R. Soc. B Biol. Sci.* 373, 20160447–20160447.
585 <https://doi.org/10.1098/rstb.2016.0447>

586 Wrangle, A.-L., Valero, J., Harkestad, L.S., Strand, Ø., Lindegarth, S., Christensen, H.T., Dolmer, P.,
587 Kristensen, P.S., Mortensen, S., 2010. Massive settlements of the Pacific oyster, *Crassostrea*
588 *gigas*, in Scandinavia. *Biol. Invasions* 12, 1453–1458. [https://doi.org/10.1007/s10530-009-](https://doi.org/10.1007/s10530-009-9565-6)
589 9565-6

590 Zhang, Guofan, Fang, X., Guo, X., Li, L., Luo, R., Xu, F., Yang, P., Zhang, L., Wang, X., Qi, H., Xiong, Z.,
591 Que, H., Xie, Y., Holland, P.W.H., Paps, J., Zhu, Y., Wu, F., Chen, Y., Wang, Jiafeng, Peng, C.,
592 Meng, J., Yang, L., Liu, J., Wen, B., Zhang, N., Huang, Z., Zhu, Q., Feng, Y., Mount, A.,
593 Hedgecock, D., Xu, Z., Liu, Y., Domazet-Lošo, T., Du, Y., Sun, X., Zhang, Shoudu, Liu, B., Cheng,
594 P., Jiang, X., Li, J., Fan, D., Wang, W., Fu, W., Wang, T., Wang, B., Zhang, J., Peng, Z., Li,
595 Yingxiang, Li, Na, Wang, Jinpeng, Chen, M., He, Y., Tan, F., Song, X., Zheng, Q., Huang, R.,
596 Yang, Hailong, Du, X., Chen, L., Yang, M., Gaffney, P.M., Wang, S., Luo, L., She, Z., Ming, Y.,
597 Huang, W., Zhang, Shu, Huang, B., Zhang, Y., Qu, T., Ni, P., Miao, G., Wang, Junyi, Wang, Q.,
598 Steinberg, C.E.W., Wang, H., Li, Ning, Qian, L., Zhang, Guojie, Li, Yingrui, Yang, Huanming, Liu,
599 X., Yin, Y., Wang, Jian, Wang, Jun, 2012. The oyster genome reveals stress adaptation and
600 complexity of shell formation. *Nature* 490, 49–54. <https://doi.org/10.1038/nature11413>

601 Zhang, G., Li, L., Meng, J., Qi, H., Qu, T., Xu, F., Zhang, L., 2016. Molecular Basis for Adaptation of
602 Oysters to Stressful Marine Intertidal Environments. *Annu. Rev. Anim. Biosci.* 4, 357–381.
603 <https://doi.org/10.1146/annurev-animal-022114-110903>

604 zu Ermgassen, P.S.E., Thurstan, R.H., Corrales, J., Alleway, H., Carranza, A., Dankers, N., DeAngelis, B.,
605 Hancock, B., Kent, F., McLeod, I., Pogoda, B., Liu, Q., Sanderson, W.G., 2020. The benefits of
606 bivalve reef restoration: A global synthesis of underrepresented species. *Aquat. Conserv.*
607 *Mar. Freshw. Ecosyst.* 30, 2050–2065. <https://doi.org/10.1002/aqc.3410>

608

609 **Acknowledgments**

610 We thank Matthias Huber, Hugo Koechlin, Jacqueline Le Grand, Bruno Petton from Argenton
611 station and the staff from Bouin station who produced the oysters used in this study. We also
612 thank Moussa Diagne who generated the algae used during experiments and Théo Gromberg
613 and Valérian Le Roy who help during field surveys. We are particularly grateful to Amandine
614 Fischer who helped optimizing telomere assays.

615 **Authors contribution.** AD, EF and CC conceived the ideas and designed methodology AD,
616 DFM, RT, CD, IQ, SP, AH, BG, EC, FP, KS, EF and CC collected the data; AD analysed the
617 data; AD led the writing of the manuscript. All authors contributed critically to the drafts and
618 gave final approval for publication.

619 **Data availability**

620 The datasets generated and the code used for analyses during the current study are available in
621 the Zenodo repository (DOI: 10.5281/zenodo.7763023).

622 **Conflict of Interest**

623 We declare no competing financial interest.

624 **Funding**

625 This work was supported by ISblue project, Interdisciplinary graduate school for the blue
626 planet (ANR-17-EURE-0015) and co-funded by a grant from the French government under
627 the program "Investissements d'Avenir" embedded in France 2030. The initiation of this
628 project and the multiple surveys of oyster cohort over years was funded by the Labex Mer
629 ("BODY" project), the "Arc Foundation for cancer research" (MOLLUSC project), and the
630 French Ministry of Agriculture and Food (ECOSCOPIA network). This work was also

631 supported by grants from Biogenouest, Infrastructures en Biologie Santé et Agronomie
632 (IBiSA) and Conseil Régional de Bretagne.

633 **Table 1.** Summarized outcomes of final selected models investigating the oyster responses to foreshore level. The table reports information on
 634 sample size, oyster cohort and age, marginal and condition r^2 , estimates (variance terms and fixed effects $\beta \pm SE$) together with test statistics.
 635 Continuous explanatory variables were previously scaled by z-score transformation to optimize model convergence. See methods section for
 636 details on statistical models and analyses.

637

Variable	Cohort	Age (month)	Final models	Model summary											
ATP content	2020	22	Food access	Number of individuals	R^2_m	R^2_c	Type	Term	$\beta (\pm SE)$	t-stat	P value				
				n = 121	0.04	-	Fixed	Intercept	66.1 \pm 5.6	11.7	0.000	**	*		
				Food access (relative to Fed) :											
								unfed	-17.0 \pm 7.9	-2.1	0.034	*			
Mitochondrial density	2020	22	Foreshore level	Number of individuals	R^2_m	R^2_c	Type	Term	$\beta (\pm SE)$	t-stat	P value				
				n = 126	0.07	-	Fixed	Intercept	1117.9 \pm 40.7	27.5	0.000	**	*		
				Foreshore level (relative to High) :											
											Middle	147.6 \pm 55.0	2.7	0.008	**
								Low	143.1 \pm 56.8	2.5	0.013	*			

rTL	2020 and 2021	8 and 22	Age	Number of individuals	R^2_m	R^2_c	Type	Term	β (\pm SE)	t-stat	P value
				n = 83	0.12	-	Fixed	Intercept	1.316 \pm 0.099	13.3	0.000 **
								Age	-0.017 \pm 0.005	-3.3	0.002 **
rTL	2020	22	Foreshore level	Number of individuals	R^2_m	R^2_c	Type	Term	β (\pm SE)	t-stat	P value
				n = 59	0.18	-	Fixed	Foreshore level (relative to High) :			
								Middle	-0.207 \pm 0.072	-2.9	0.006 **
								Low	-0.238 \pm 0.073	-3.2	0.002 **
Filtration rate	2020	17	Weight + days starved + temperature + temperature ² + Foreshore level + temperature ² × Foreshore level + (1 Oyster ID)	Number of individuals	R^2_m	R^2_c	Type	Term	Variance		
				n = 52	0.62	0.74	Random	Oyster ID	0.16		
								Residual	0.23		
									β (\pm SE)	t-stat	P value
							Fixed	Intercept	-0.62 \pm 0.24	-2.52	0.013
								Weight	0.30 \pm 0.03	10.9	0.000 **
								Days starved	-0.05 \pm 0.03	-2.0	0.046 *

Temperature	0.11 ± 0.02	4.9	0.000	** *
Temperature ²	-0.002 ± 0.001	-4.8	0.000	** *
Foreshore level (relative to High) :				
Middle	0.28 ± 0.11	2.6	0.014	*
Low	0.36 ± 0.11	3.3	0.002	**
Temperature ² x Foreshore level:				
Temperature ² x Middle	-1.8·10 ⁻⁴ ± 1.5·10 ⁻⁴	-1.2	0.224	
Temperature ² x Low	-4.2·10 ⁻⁴ ± 1.5·10 ⁻⁴	-2.8	0.006	**

Maximum metabolic rate	2020	17	Weight + temperature + Foreshore level + temperature x Foreshore level + (1 Oyster ID)	Number of individuals	R^2_m	R^2_c	Type	Term	Variance		
				n = 52	0.86	0.90	Random	Oyster ID	0.09		
								Residual	0.14		
									β (± SE)	t-stat	P value
							Fixed	Intercept	-2.2 ± 0.07	-32.5	0.000 ** *
								Weight	0.21 ± 0.02	13.3	0.000 ** *
								Temperature	0.06 ± 0.00	20.7	0.000 ** *
								Foreshore level (relative to High) :			

Middle	0.34 ± 0.10	3.4	0.001	**
Low	0.55 ± 0.10	5.5	0.000	** *

Temperature x
Foreshore level:

Temperature x Middle	-0.006 ± 0.004	-1.5	0.143	
Temperature x Low	-0.013 ± 0.004	-3.3	0.001	**

638

639

640 **Figure captions**

641 Figure 1. Schematic illustration of oyster production and experimental design. A) Wild spats
642 are collected every year at the Aix Island (46°0'51N, 1°9'39W) to enrich a captive brood
643 stock of a diversified gene pool from the same population. These individuals are exposed to
644 natural conditions at the Aber Benoît (48°34'30N, 4°36'18W) for up to 10 years. B) Each
645 summer, we pool gametes of ca. 100 reproductive adults in laboratory to produce a cohort of
646 captive spats. C) At 7 month old, 2,700 captive spats are distributed in the field along
647 foreshore levels. Due to month variation of tidal range, oysters at Low shore (blue star) are
648 exposed 80% of their time to sea water, approaching subtidal conditions. Instead, oysters from
649 High shore (yellow star) are submerged only during strong tidal range, spending only 20% of
650 their time submerged. Oysters from Middle shore (grey star) are exposed half of their time to
651 sea water. We sampled oyster of different cohorts for investigating physiological adjustments
652 as described in the text. Picture copyrights fall to Andréaz Dupoué, Stéphane Pouvreau (larva
653 lifecycle) and the Ifremer.

654

655 Figure 2. Multivariate analyze of inter-individual proteomic profiles of oysters from High
656 (yellow), Middle (grey) or Low (blue) shores regarding the relative expression of chaperone
657 proteins, and those involved in oxidative status. This principal component analysis
658 discriminate the three foreshore levels (ellipse of 95% confidence interval), along the first axe
659 (horizontal) given that High shores oysters experienced enhanced antioxidant shielding
660 compared to Low shore individuals. Abbreviations : Heat Shock Protein (HSP), NAD(P)H
661 oxidase (NOX), Catalase (CAT), Non-selenium Glutathione Peroxidase (Non-Se GPx),
662 peroxidase YfeX (YfeX), peroxiredoxin 5 (PRDX5), superoxide dismutase (SOD),
663 Glutathione Peroxidase (GPx), Peptide methionine R S oxide reductase (PMRS).

664

665 Figure 3. Additive effects of foreshore level and food access on energetic efficiency. A) Fed
666 oysters (open dots) showed higher ATP concentration than unfed individuals (closed dots)
667 regardless of foreshore level, although B) haemocytes in oysters from High shore (yellow
668 dots) had lower mitochondrial density than those from Middle (grey dots) and Low shores
669 (blue dots). Significant effects of foreshore level on ATP concentration and mitochondrial
670 density are symbolized: * $p < 0.05$, and n.s. (non-significant).

671

672 Figure 4. Effects of oyster age class and foreshore level on variation in relative telomere
673 length. Telomeres were shorter in older oysters, in addition to an environmental effect related
674 to foreshore level. On average, oysters from High shore (yellow dot and line) exhibited longer
675 telomeres than individuals from Middle (grey dot and line) and Low shores (blue dot and
676 line).


677

678 Figure 5. Impacts of foreshore level on the temperature dependence of A) filtration rate and
679 B) maximum metabolic rate (estimated through VO_2 in feeding oysters). Filtration rate did not
680 differ between foreshore levels, while temperature dependence of metabolic rate was stronger
681 in oysters from High shore (yellow symbols and lines), compared to those of Middle (grey
682 symbols and lines) and Low shores (blue symbols and lines). Data are mass-adjusted values
683 (residuals from linear relationship between log-transformed filtration or VO_2 and oysters
684 weight) and best linear regression fits with prediction intervals.

685

A) Brood stock collection


Field site 1:
Spat collection



Standardized gene pool

➔

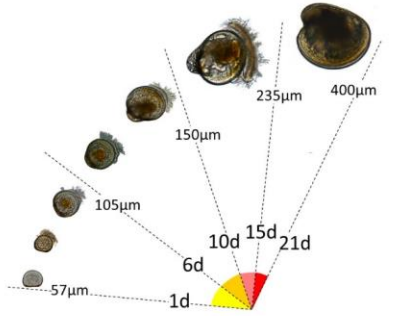
Field site 2:
Growing 1 - 10 years



Reproductive adults

B) Reproduction

Laboratory (n = 100 adults/year):
Fecundation & early development



(n = 1 cohort/year)


C) Field experimentation

n = 2 700 juveniles/cohort

Time spent submerged

Foreshore level

High Middle Low



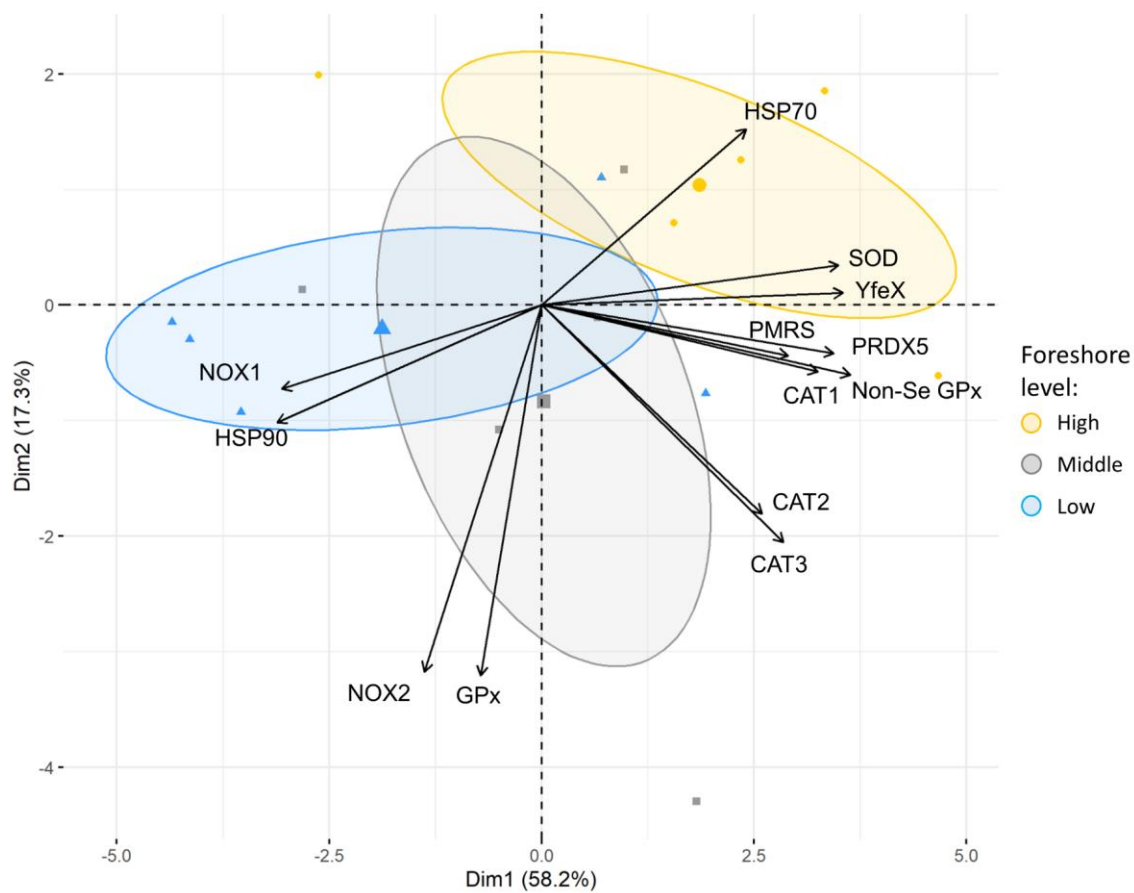
Sampling strategy:

Measures	Acclimatization time to foreshore level (month)	Oyster age (month)
Oxidative response	2	9
Cellular energetics	15	22
Telomere length	15	22
Physiological norms	10	17

687

688

689 Figure 2.

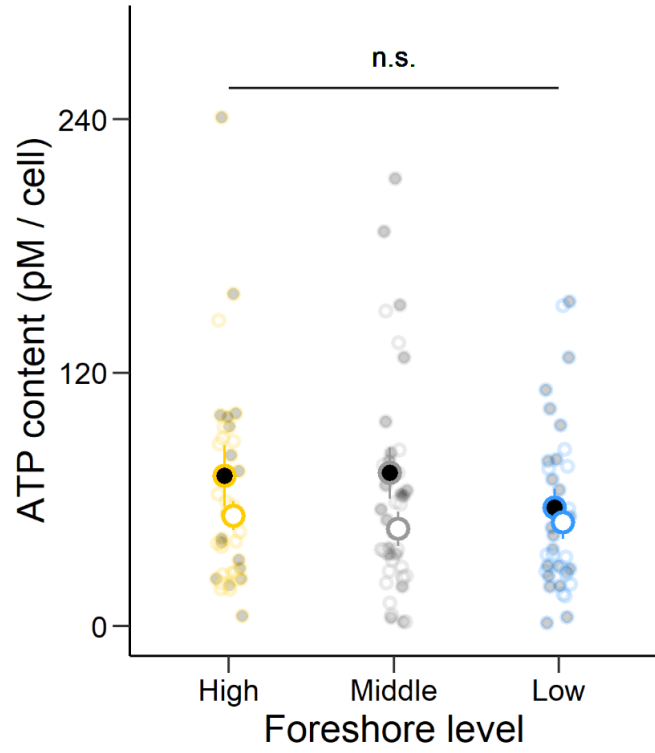


690

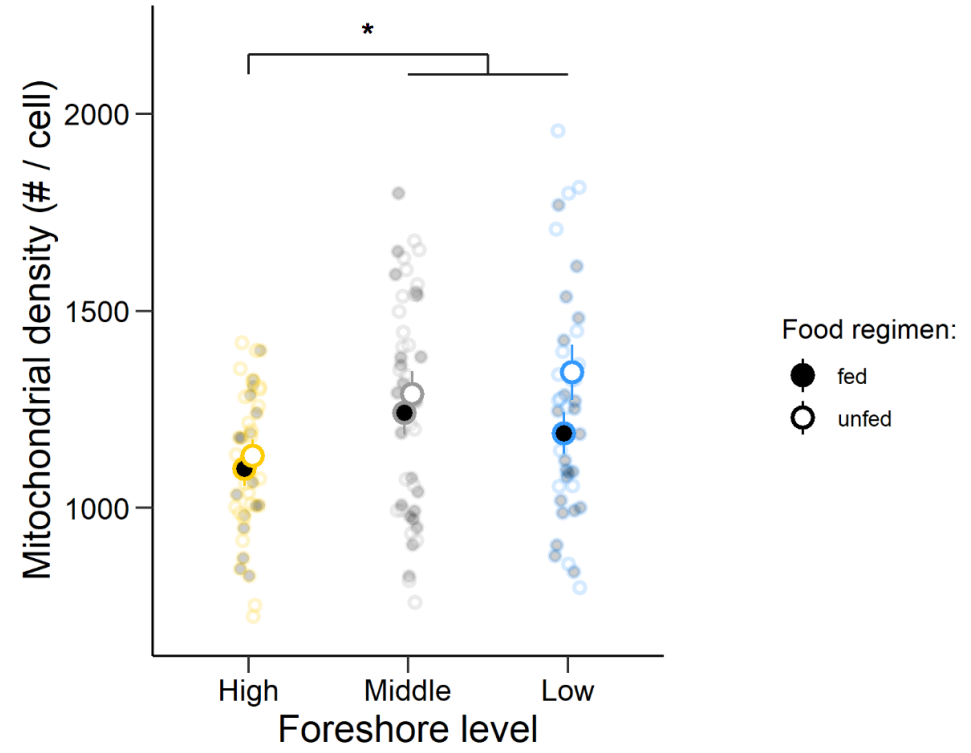
691

692 Figure 3.

A)

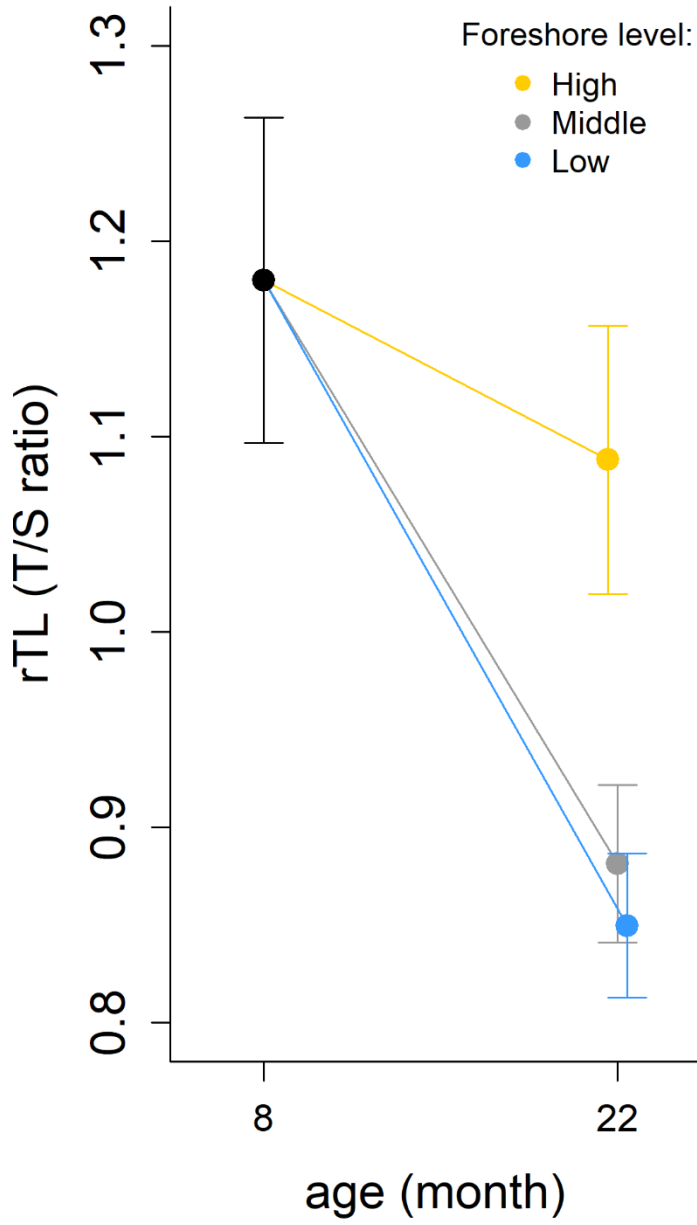


B)



693

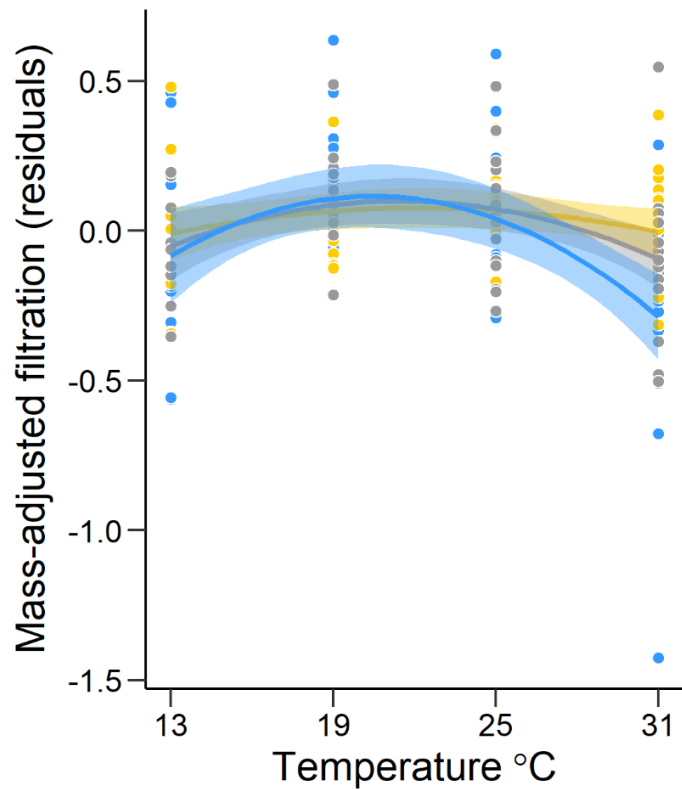
694 Figure 4.



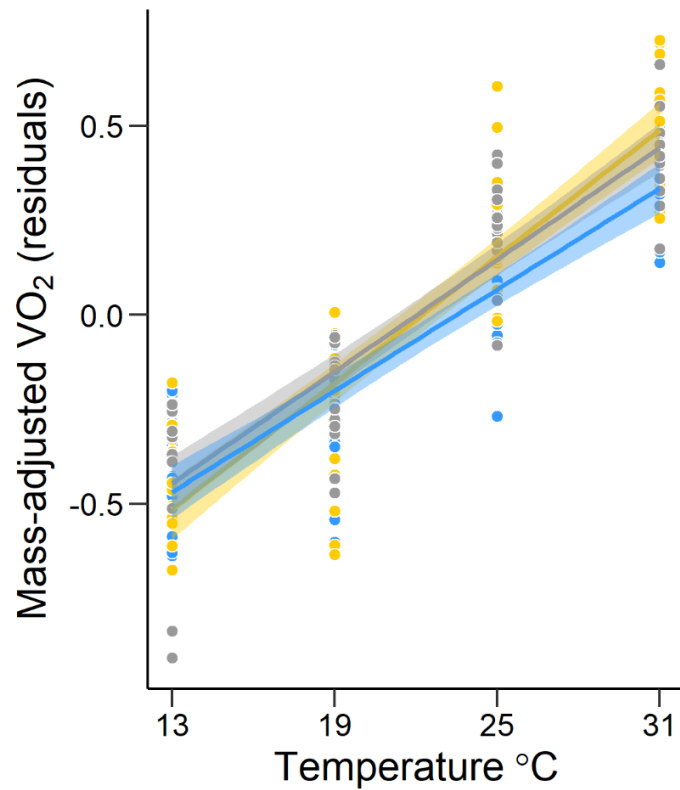
695

696

A)



B)



Foreshore level:

- High
- Middle
- Low